3. Margarida BELO PEREIRA : "Improving the assimilation of water in a NWP model"

1. Introduction

The basic equation for analysis is :

$$x^{a} = x^{b} + K(y - Hx^{b}), \qquad K = BH^{\mathrm{T}}(HBH^{\mathrm{T}} + R)^{-1}$$

where x^b is the background field, x^a is the analysis field, y is the observation vector, H is the forward interpolation operator, R is the observation error covariance matrix and B is the background error matrix.

The role of B matrix is to spread the observation departures both in vertical and horizontal. Therefore, the accuracy of the B matrix is very important for the analysis quality.

In the present work, the B matrix is determined using the Analysis Ensemble Method (Belo Pereira, 2002).

2. Estimation of the length scale of auto-covariance

Using the Helmholtz's theorem, we obtain the rotational part of the meridional wind, $v^{\Psi}=\partial\Psi/\partial x$. So, the covariance of v^{Ψ} between two points is given by

$$\langle v_1^{\Psi}\ v_2^{\Psi}\rangle = \langle \frac{\partial\Psi_1}{\partial x_1}\frac{\partial\Psi_2}{\partial x_2}\rangle = \frac{\partial^2\langle\Psi_1\ \Psi_2\rangle}{\partial x_1\ \partial x_2}$$

and covariance of the streamfunction (Ψ) can be expressed as function of its auto-correlation function ρ and of its variances $\sigma(\Psi_1)$ and $\sigma(\Psi_2)$ respectively at points 1 and 2 :

$$\langle \Psi_1\ \Psi_2\rangle = \sigma(\Psi_1)\ \sigma(\Psi_2)\ \rho$$

deriving this expression,

$$\frac{\partial^2\langle\Psi_1\Psi_2\rangle}{\partial x_1\ \partial x_2} = \frac{d\sigma(\Psi_1)}{dx_1}\frac{d\sigma(\Psi_2)}{dx_2}\rho + \sigma(\Psi_1)\ \sigma(\Psi_2)\ \frac{\partial^2\rho}{\partial x_1\partial x_2} + \sigma(\Psi_1)\ \frac{d\sigma(\Psi_2)}{dx_2}\frac{\partial\rho}{\partial x_1} + \frac{d\sigma(\Psi_1)}{dx_1}\ \sigma(\Psi_2)\ \frac{\partial\rho}{\partial x_2}$$

Defining $x'=x_1-x_2$, we can assume that the first derivative of ρ vanishes at $x'=0$ (this assumption is reasonable since ρ is maximum at $x'=0$ and decreases as the distance from the origin increases).

And using the definition of length scale (Daley, 1991) for the one-dimensional case

$$\left(L_x^{\Psi}\right)^2 = -\left(\rho\Big/\frac{d^2\rho}{dx'^2}\right)_{x'=0}$$

we obtain the length scale for the streamfunction auto-covariance:

$$\left(L_x^{\Psi}\right)^2 = \sigma^2(\Psi)\Bigg/\left[\sigma^2\left(\frac{\partial\Psi}{\partial x}\right) - \left(\frac{\partial\sigma(\Psi)}{\partial x}\right)^2\right]$$

The length scale defined according to Daley (1991) gives an idea about how the auto-correlation function decays with distance from its initial value.

3. Experiments description

The background error statistics were estimated for three datasets of differences between 6 h forecasts. In the first set (called *metropole*) the background errors come from the differences between two 4d-var cycles of ARPEGE with spectral truncation T298 and stretching factor (c) equal to 3.5. The second set (denominated *tropic*) uses two 4d-var cycles of ARPEGE with truncation T299 and constant resolution (c=1). The observations used for this set include pseudo-observations of tropical cyclones ("bogus" observations). In both *metropole* and *tropic* sets, the uncertainties are caused only by the perturbations in the observations (see Belo Pereira, 2002). So it is assumed that the model is perfect and the background errors are only due to the propagation of observations uncertainties. The third set (called *arpf_arpt*) uses one experiment with constant resolution and another one with c=3.5 . So in the last set the model is not considered as perfect any more and it is considered that the background error is also related with the horizontal resolution.

The background differences come from 6 h forecasts valid at 18 h UTC, during the period between 4th of February and 14th of March, 2002.

4.1 Results: Statistics in spectral space

On average, the largest vorticity background errors are found in the high troposphere, for wavenumbers between 30 and 70, for all experiments, but the error magnitude is significantly larger for the *arpf_arpt* set (figures 1 and 2). On the other hand, the smallest errors occur for the *metropole* set, with a maximum is shifted towards larger scales relatively to the *tropic* set.

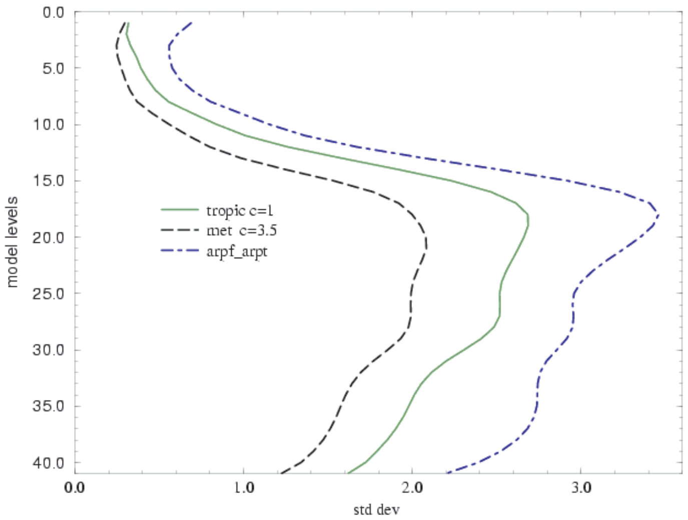

Figure 1 - Vertical profile of standard deviation ($10^{-5}s^{-1}$) for vorticity background error.

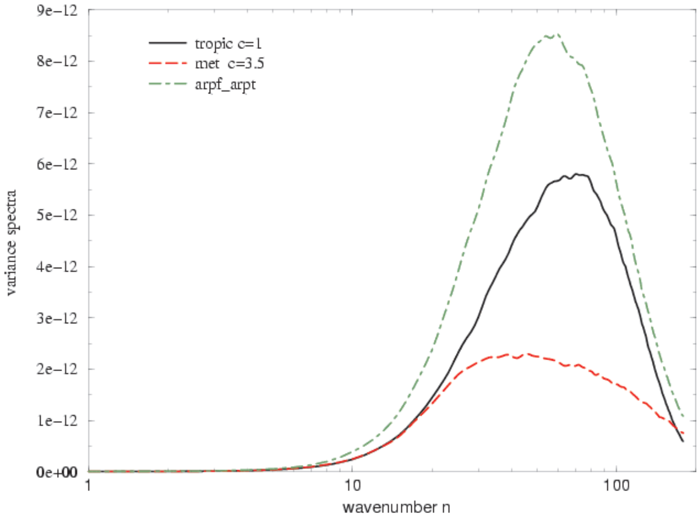

Figure 2 - Variance spectrum for vorticity for model level 21 (near 500 hPa).

The surface-pressure background errors are significantly larger when computed using the *arpf_arpt* set than with other sets. The largest differences occur for synoptic scales, for wavenumbers between 5 and 20 (figure 3). The same result is found for temperature and specific humidity errors.

The variance spectrum of streamfunction background error is very similar for both *tropic* and *metropole* datasets. This result can be explained by the fact that the largest contributions for the streamfunction background errors come from the planetary scales (figure not shown). The results show also that with the *arpf_arpt* set the error variance is larger than with the other datasets.

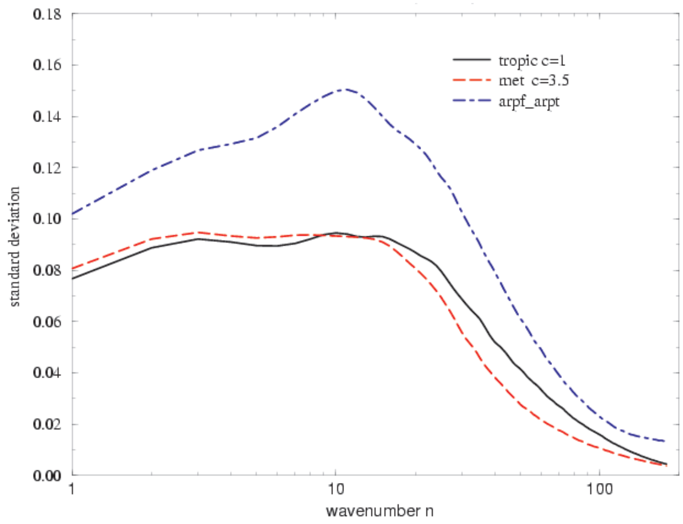

Figure 3 - Standard deviation (hPa) spectrum of surface pressure background error.

4.2 Results: Statistics in gridpoint space

For the *metropole* set, the largest surface-pressure background errors are found near the North Pole, to the North of Russia. Moreover large errors occur in the extra-tropics on oceans (fig. 4a). So the larger errors occur in the areas of larger surface-pressure variability and in data void areas, which seems reasonable. For the *tropic* set, the errors around the North Pole are reduced, comparing to the *metropole* set. On the other hand, the magnitude of the background errors in the extra-tropical Pacific ocean is increased here. It is also worthwhile to notice that the largest errors for the *tropic* set are found in the tropical Indian ocean, due to the use of "bogus" observations (fig. 4b). This shows the sensitivity of the Ensemble Method to the observations used during the assimilation cycle. For the *arpf_arpt* (figure not shown), the spatial distribution of the errors is very similar to the one obtained with the *tropic* set. However, in this case local maxima are found in Andes, Himalayas regions and near the North Pole to the North of Russia. Moreover, for the *arpf_arpt*, the magnitude of background errors is also significantly increased over the southern extra-tropical Pacific ocean, tropical Indian ocean and over the North Atlantic ocean, comparatively to the other two datasets.

For the *metropole* set, the vorticity background errors are concentrated in the high resolution areas, having very small values in the regions where the equivalent truncation is larger than 500. This result can be explained by the fact that the largest contributions for such errors come from the small scales (see fig. 2). On the other hand, for the *tropic* set, the largest errors are located in extra-tropical regions over the oceans, over Himalaya and over the North Pole. For the *arpf_arpt* set, the error magnitude is increased everywhere (when comparing with the *tropic* set), but this increase is stronger over North Atlantic and Europe. This result is due to the fact that the difference in resolution between the two runs used in this dataset is larger in these regions.

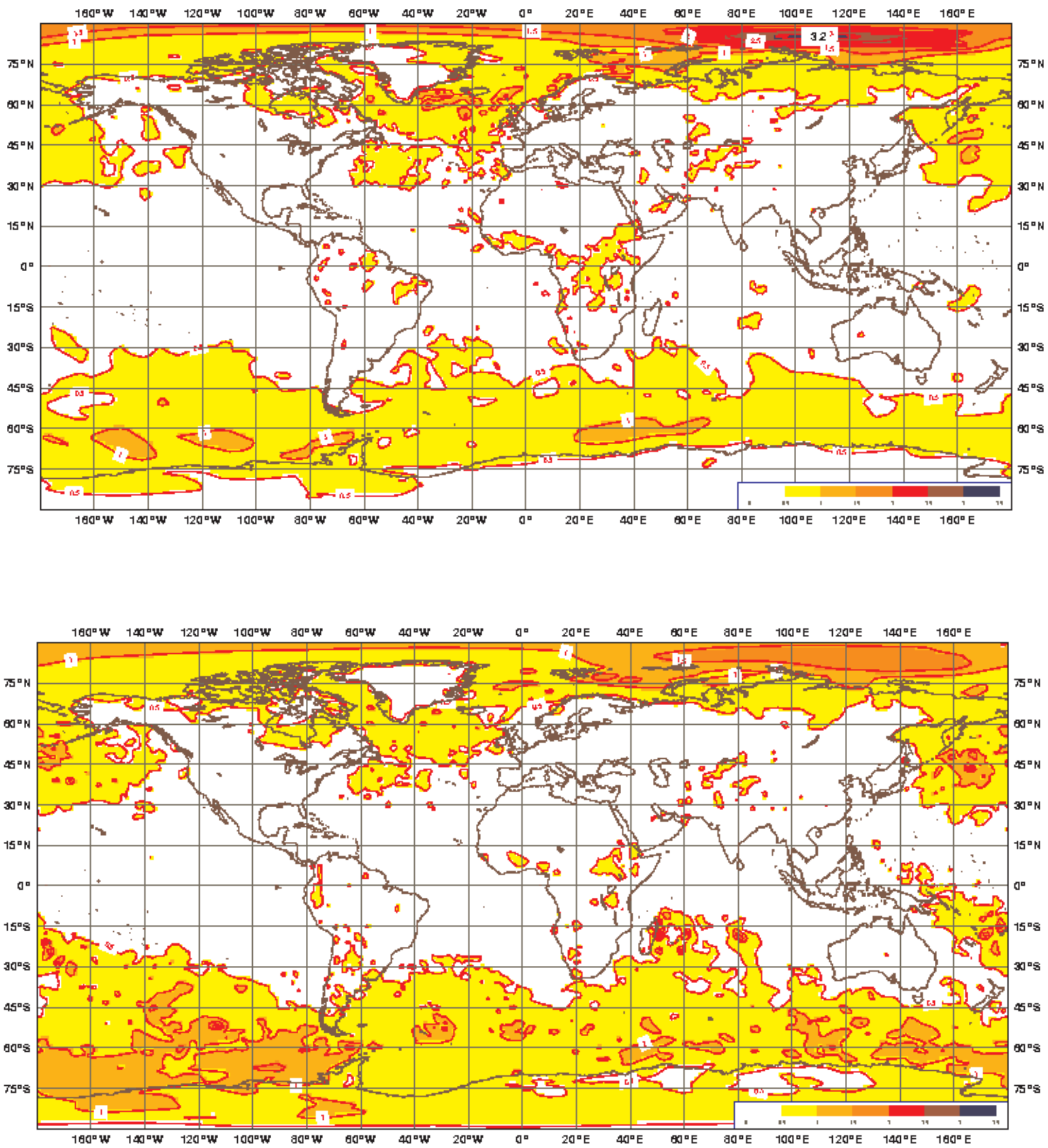

(a)

(b)

Figure 4 - Standard deviation (hPa) of surface-pressure background error :
(a) *metropole* set and (b) *tropic* set.

Applying the method described in section 2 to calculate the length scale of auto-correlations, we verified that for the *metropole* set the length scale tends to increase towards the coarser resolution areas (figures not shown), while for the *tropic* data set, the auto-correlation functions tend to be broader in the tropics (larger length-scales) than in middle and high latitudes (see fig. 6 for zonal wind near 500 hPa). Moreover, the results show that the meridional length-scale is more homogenous (less dependent on the geographical localization) than the zonal length-scale.